

RESEARCH ARTICLE

Nanoparticulate matter exposure results in neuroinflammatory changes in the corpus callosum

Robin Babadjouni¹ , Arati Patel¹ , Qinghai Liu¹, Kristina Shkirkova¹, Krista Lamorie-Foote^{1*} , Michelle Connor¹, Drew M. Hodis¹, Hank Cheng⁴, Constantinos Sioutas³, Todd E. Morgan⁴, Caleb E. Finch⁴, William J. Mack^{1,2}

1 Zilkha Neurogenetic Institute, Keck School of Medicine, University of Southern California, Los Angeles, California, United States of America, **2** Department of Neurosurgery, Keck School of Medicine, University of Southern California, Los Angeles, California, United States of America, **3** Department of Civil and Environmental Engineering, Viterbi School of Engineering, University of Southern California, Los Angeles, California, United States of America, **4** Leonard Davis School of Gerontology, University of Southern California, Los Angeles, California, United States of America

 These authors contributed equally to this work.

* lamorief@usc.edu



 OPEN ACCESS

Citation: Babadjouni R, Patel A, Liu Q, Shkirkova K, Lamorie-Foote K, Connor M, et al. (2018) Nanoparticulate matter exposure results in neuroinflammatory changes in the corpus callosum. *PLoS ONE* 13(11): e0206934. <https://doi.org/10.1371/journal.pone.0206934>

Editor: Alexander Larcombe, Telethon Institute for Child Health Research, AUSTRALIA

Received: July 3, 2018

Accepted: October 21, 2018

Published: November 5, 2018

Copyright: © 2018 Babadjouni et al. This is an open access article distributed under the terms of the [Creative Commons Attribution License](https://creativecommons.org/licenses/by/4.0/), which permits unrestricted use, distribution, and reproduction in any medium, provided the original author and source are credited.

Data Availability Statement: All relevant data are within the paper and its Supporting Information files.

Funding: This study was supported by a grant awarded to WJM through the National Institutes of Health (NIH)/National Institute of Environmental Health Science (NIEHS): grant #R01ES024936, URLs: nih.gov and niehs.nih.gov. CEF was supported by the NIH: grant #R01AG051521 and the NIH/National Institute on Aging (NIA): grant #R21AG050201. The study was supported by the

Abstract

Epidemiological studies have established an association between air pollution particulate matter exposure (PM_{2.5}) and neurocognitive decline. Experimental data suggest that microglia play an essential role in air pollution PM-induced neuroinflammation and oxidative stress. This study examined the effect of nano-sized particulate matter (nPM) on complement C5 deposition and microglial activation in the corpus callosum of mice (C57BL/6J males). nPM was collected in an urban Los Angeles region impacted by traffic emissions. Mice were exposed to 10 weeks of re-aerosolized nPM or filtered air for a cumulative 150 hours. nPM-exposed mice exhibited reactive microglia and 2-fold increased local deposition of complement C5/ C5α proteins and complement component C5a receptor 1 (CD88) in the corpus callosum. However, serum C5 levels did not differ between nPM and filtered air cohorts. These findings demonstrate white matter C5 deposition and microglial activation secondary to nPM exposure. The C5 upregulation appears to be localized to the brain.

Introduction

Exposure to air pollution particulate matter (PM) is a potent generator of neuroinflammation in the central nervous system (CNS) [1, 2] and has been associated with decreased white matter volume and reduced cognition in older adults [3–5]. Murine studies suggest that particulate matter exposure results in myelin loss in the CA1 stratum oriens of young mice, consistent with myelin reduction classically evident with aging [6]. While multiple CNS cell types are implicated in the inflammatory response, microglia have critical roles in particulate matter-induced CNS injury [7]. Under physiologic conditions, microglial activation enables homeostatic phagocytosis and facilitates synaptic remodeling and brain maturation. These phagocytic

University of Southern California Alzheimer Disease Research Center (National Institutes of health grant: #P50AG05142). The funders had no role in the study design, data collection and analysis, decision to publish, or preparation of the manuscript.

Competing interests: The authors have declared that no competing interests exist.

mechanisms, however, are aberrantly triggered in a host of disease processes [8]. Studies have demonstrated that macrophages and microglia contribute to white matter injury in the setting of multiple sclerosis[9], periventricular leukomalacia, and amyotrophic lateral sclerosis[10]. Microglia propagate neuroinflammation through expression of pro-inflammatory cytokines and generation of reactive oxygen species[11]. When activated, microglia produce complement proteins[12, 13] and express complement-specific receptors, particularly C5aR (CD88) [12, 14–16]. In vitro studies of activated microglia demonstrate adherence and cytotoxicity to oligodendrocytes in the presence of complement factors[17]. The complement cascade, and principally the C5 anaphylatoxin, may play an important role in the pathogenesis of white matter inflammation following nanoparticulate matter (nPM) exposure.

This investigation examines the association between nPM exposure and white matter (corpus callosum) C5 deposition in a murine model. Immunohistochemical analysis and ELISA studies explore the relationship between complement upregulation and the presence of reactive microglia.

Materials and methods

Protocol

All procedures utilized in this study were approved by the Institutional Animal Care and Use Committee (IACUC; protocol # 20235) of the University of Southern California and carried out in accordance with the Guide for the Care and Use of Laboratory Animals (NIH). All mice were male C57BL/6J mice (15–16 weeks of age; 24–29g) and housed in a barrier facility with free access to food and water on a 12-hour light dark cycle, except during the nPM/ filtered air exposures. The mice did not have access to food and water during the daily five-hour exposure periods.

Particulate matter collection. Collection of nPM (particles smaller than 0.2 μm in diameter) was conducted in an urban area in central Los Angeles, impacted mostly by traffic emissions[18, 19]. Briefly, urban nPM (aerodynamic diameter <200 nm) is collected at 400 L/min flow using a high-volume ultrafine particle sampler[19]. The sampler incorporates an ultrafine particle multiple rectangular (slit) geometry jet conventional impactor that removes particles larger than 0.2 μm , and the remaining nPM is collected on pretreated Teflon filters (8x10", PTFE, 2 μm pore) and transferred into an aqueous suspension by 30 min soaking of filters in Milli-Q deionized water (resistivity, 18.2 MW; total organic compounds <10 ppb; particle free; endotoxin levels <1 units/mL; endotoxin-free glass vials), followed by vortexing (5 min) and sonication (30 min) for resuspension. No endotoxin is detected in these suspensions (*Limulus*amebocyte assay: LPS <0.02 EU/ml). As a control, fresh sterile filters were sham extracted and stored. Aqueous nPM suspensions were pooled and frozen as a stock at -20°C , following recommended procedures by the US EPA, which show retention of chemical stability for ≥ 3 mo[20].

For mouse exposure, the nPM were re-aerosolized by an atomizer using compressed particle-free filtered air as discussed in detail in previous publications [1, 19]. During mouse exposure, the particle size and concentration were continuously monitored by a scanning mobility particle sizer (SMPS model 3080; TSI Inc., Shoreview, MN) in parallel with the animal exposure chambers. We maintained the average nPM mass concentration at approximately 330 (± 25) $\mu\text{g}/\text{m}^3$ - roughly twice that of busy roadways [21]. From the total of 15 l/min of aerosol flow generated, the majority (10 l/min) was drawn through the exposure chamber. The remaining 5 l/min was diverted to filters for particle collection and characterization. Teflon and quartz filters, sample concurrently the aerosol during exposure. The mass concentration of the nPM was determined by pre- and post- weighing the Teflon filter under controlled

temperature and relative humidity. Inorganic ions [ammonium (NH_4^+), nitrate (NO_3^-), sulfate (SO_4^{2-})] were analyzed by ion chromatography, and PM-bound metals/ trace elements were assayed by magnetic-sector inductively coupled plasma mass spectroscopy. Water-soluble organic carbon collected on the quartz filter was assayed by a GE-Sievers liquid analyzer (GE-Sievers, Boulder, CO). More details about the inorganic and organic compound contents of these samples have been previously described[1]. Exposures were conducted in temperature and air controlled sealed whole-body exposure chambers with adequate ventilation to minimize buildup of animal-generated contaminants[1, 22, 23].

Particulate matter exposures. Mice were group-housed with four mice in each cage and randomized to re-aerosolized nPM or filtered air exposure cohorts. Exposures occurred for five hours/day, three-days/ week for a 10-week period. The mice were humanely euthanized 72 hours after the last exposure. While under anesthesia with ketamine (80 mg/kg IP) and xylazine (10 mg/kg IP), serum (up to .22ml) was collected via a direct cardiac puncture. The mice were then transcardially perfused with PBS and heparin (5 U/mL) saline followed by a fixative solution (4% paraformaldehyde and .2% picric acid in .1 mol/L phosphate buffer). The brains were harvested and stored in paraformaldehyde for 24 hours at 4°C. Tissue was then dehydrated in ethanol (70%) and sent to pathology for paraffin embedding.

Immunohistochemistry. Immunohistochemical analysis was performed on paraffin embedded brain sections as described below:

Slides were deparaffined, and hydrated using a series of different alcohol concentrations (ranging from 100% to 70%). Antigen was retrieved with Dako target retrieval solution, dipped in 3% H_2O_2 for 10 min, and then blocked with serum. Slides were incubated overnight with a rabbit anti- glial fibrillary acidic protein (GFAP) antibody (diluted 1:10 000; Dako, Denmark) or a rabbit anti-ionized calcium-binding adapter molecule 1 (IBA1) antibody (1:200; Wako, Japan). Subsequently, sections were treated with the appropriate biotinylated secondary antibody Vectastain Elite ABC kit (Vector Laboratories, Burlingame, California, USA) and visualized with diaminobenzidine (DAB). A LAS AF microscope (Leica, Germany) was used to capture images of the immunostained slices. NIH Image J software was employed to quantify the optical density of DAB signal for analysis (rsbweb.nih.gov/ij/). The number of GFAP and IBA-1 positive cells in one high powered field (40x) were counted in the left medial and right medial corpus callosum and the two values subsequently averaged. IBA-1/GFAP cells that exhibited double immunopositivity with DAPI were only counted. For IBA-1 analysis, only heavily stained cells larger than 5 μm were counted. Separately, mean cell density of IBA-1/GFAP positive cells was counted in the left medial and right corpus callosum and the two values were subsequently averaged. To assess microglia morphology, images were evaluated using Image J software following a protocol previously described [24]. Briefly, the corpus callosum was selected and the “Adjust Threshold” function was applied as the intensity threshold. Total cell size was measured at this intensity threshold without a size filter. Cell body size was measured by lowering the threshold 5 points and applying a size filter of 100 pixels using the “Analyze Particles” function. To calculate the overall size of the dendritic processes, cell body size was subtracted from total cell size. From this, the cell body to dendritic process size ratio was calculated.

Immunofluorescence. Similar to the protocol for IBA-1 and GFAP staining, slides were deparaffined, and hydrated using a series of alcohol concentrations (ranging from 100% to 70%). Antigen retrieval was achieved with Dako target retrieval solution, dipped in 3% H_2O_2 for 10 min, and then blocked with 5% donkey serum. Slides were incubated overnight with anti-C5 (mouse 1:50 Hycult Biotech, Netherlands; clone BB5.1), anti-CD88 (rat 1:200 Hycult Biotech, Netherland; HM1076) or rabbit complement component C5 α (125kDa) antibody (1:50 Santa Cruz, SC-21941). Subsequently, sections were washed, incubated with secondary

antibodies (Alexa Fluor 568, Invitrogen, Carlsbad, CA) for one hour, and nuclei were stained with DAPI (Invitrogen) for 10 minutes. Slides were mounted with Dako fluorescent mounting media, coverslipped, and then visualized using Zeiss 510 confocal microscopy and BZ-9000 fluorescent microscopy (Keyence, NJ). NIH Image J software was used to quantify immunofluorescence. The images were converted to 8-bit and adjusted to threshold to count the positive cells. Mean density area for C5, C5 α and CD88 was measured in one high powered field (C5: 400x, C5 α : 400x, CD88:200x) in the left and right medial corpus callosum and the two values were averaged. Protocols followed the NIH Image J user guide.

Double immunofluorescence staining was carried out following a similar protocol to what was described above. Slides were incubated overnight with mouse anti-C5 (diluted 1:50, Hycult Biotech, Netherlands, HM1073) and one of the three primary antibodies: 1) rabbit anti-gial fibrillary acidic protein (GFAP) (diluted 1:10,000, Dako, Denmark), 2) rabbit anti-ionized calcium-binding adapter molecule 1 (IBA1) antibody (1:200; Wako, Japan), or 3) rabbit anti-choline acetyltransferase (ChAT) antibody (diluted 1:150, MilliporeSigma, Germany). ChAT is a marker for choline acetyltransferase and can be used to identify cholinergic neurons [25]. Sections were then washed and incubated for one hour with one of the three secondary antibody solutions based on the previous primary antibody solution: 1) Alexa Fluor 800 and Alexa Fluor 647, 2) Alexa Fluor 800 and Alexa Fluor 647, or 3) Alexa Fluor 568 and Alexa Fluor 647 (Invitrogen, Carlsbad, CA). Nuclei were stained with DAPI (Invitrogen), slides were mounted with mounting media, and subsequently imaged following the above protocol. Three images were taken with different channels to visualize the different stains. NIH Image J software was used to merge the images using the "Image Calculator" function.

ELISA analysis. Serum was obtained by direct cardiac puncture at the time of euthanasia from nPM and filtered air groups. ELISA was performed for C5 (μg C5 protein/ mg total protein) and TNF-alpha (μg TNF-alpha protein/ mg total protein) according to manufacturer's instructions (C5; Kamiya Biomedical Company, KT- 11775, Seattle, WA) (TNF-alpha; R&D Systems P134505, Minneapolis, MN).

Statistical analyses

The differences between nPM and filtered air cohorts were analyzed with two-tailed unpaired Student's t-tests. Data in the text are presented as mean \pm standard deviation. $P \leq .05$ is considered statistically significant.

Results

The mass concentration during the 150 hours of the exposure was 330 (± 25) $\mu\text{g}/\text{m}^3$ whereas the number concentration was 1.6 (± 0.3) $\times 10^5$ particles/ cm^3 . Total Organic Carbon (TOC) was the most predominant chemical species, accounting for 68 (± 9)% of the total mass. The mass fractions of other trace elements and metals (in units of $\text{ng}/\mu\text{g}$ of PM mass) are listed in the table below (Table 1). The size distribution of the exposure aerosol is presented below (Table 2) and is typical of particulate matter in an urban area impacted by traffic emissions[1].

Reactive microglia (IBA-1) and astrocytes (GFAP)

IBA-1 cell counts in the medial corpus callosum were increased 30% by exposure to nPM: filtered air (67.3 ± 23.6 , $n = 8$) and nPM mice (86.9 ± 9.4 , $p = 0.047$, $n = 8$) (Fig 1A and 1B). However, no differences existed in the medial corpus callosum for GFAP cell counts between filtered air (85.5 ± 13.2 , $n = 8$) and nPM mice (85.6 ± 11.0 , $p = 0.98$, $n = 8$) (Fig 1D and 1E). Further, IBA-1 cell density in the medial corpus callosum was increased 25% by exposure to nPM: filtered air (140.2 ± 7.9 , $n = 8$) and nPM mice (177.9 ± 4.1 , $n = 8$, $p < 0.001$). No

Table 1. Mass fractions of trace elements and metals (ng/μg of PM mass) during exposure.

Metal / Trace Element	Mass Fraction
Na	36.88 ± 0.46
Mg	10.34 ± 0.02
Al	8.85 ± 0.04
S	37.69 ± 0.27
K	6.67 ± 0.07
Ca	33.28 ± 0.35
Ti	0.35 ± 0.04
V	0.04 ± 0.00
Cr	0.16 ± 0.00
Mn	0.33 ± 0.00
Fe	8.65 ± 0.07
Ni	0.26 ± 0.01
Cu	0.58 ± 0.01
Zn	2.98 ± 0.02
Pb	0.11 ± 0.00

<https://doi.org/10.1371/journal.pone.0206934.t001>

differences in cell density existed in the medial corpus callosum for GFAP cell density between filtered air (178.3 ± 5.9 , $n = 8$) and nPM mice (179.3 ± 8.4 , $p = 0.78$, $n = 8$). IBA-1 cell body to dendritic process size ratio was significantly increased following nPM exposure (1.25 ± 0.27 , $n = 8$) compared to filtered air (0.68 ± 0.27 , $p < 0.001$, $n = 8$) (Fig 1C).

Complement deposition and receptor expression: C5, C5α, CD88

Exposure to nPM caused 2-fold increases in C5 (Fig 2A–2C) and C5α (Fig 2D–2F) integrated density staining in the corpus callosum between mice in the filtered air (C5: 6.3 ± 2.2 ; C5α 1.8 ± 0.60 , $n = 8$) and nPM groups (C5: 10.7 ± 2.5 , $p = 0.001$; C5α: 3.96 ± 2.2 , $p = 0.02$, $n = 8$). CD88 increased by 15% in the medial corpus callosum (Fig 2G–2I) between filtered air (14.9 ± 3.4 , $n = 18$) and nPM mice (17.3 ± 3.6 , $p = 0.04$, $n = 18$).

There was co-localization of C5 and ChAT (Fig 3C). There was a scattering of C5 on and nearby IBA-1 (Fig 3A) and GFAP positive cells (Fig 3B).

Serum TNF-alpha levels and Serum C5 levels

Serum ELISA C5 values (ng/mg total protein) did not significantly differ between filtered air (32.4 ± 4.8 , $n = 8$) and nPM mice (31.6 ± 6.6 , $p = 0.79$, $n = 8$). See Fig 4A. However, Serum ELISA TNF-alpha values (ng/mg total protein) were elevated 28% in nPM mice (2.4 ± 0.50 , $n = 8$) compared to filtered air mice (1.9 ± 0.5 , $p = 0.04$, $n = 7$) (Fig 4B).

Table 2. Size distribution of the exposure aerosol.

	Mean	Std. Dev.
Median (nm)	55.2	0.6
Mean (nm)	68	0.7
Geo. Mean (nm)	55.9	0.5
Mode (nm)	53.3	3.9
Geo. Std. Dev.	1.8	
Total Concentration (particles/cm ³)	3.9E+05	3.3E+03

<https://doi.org/10.1371/journal.pone.0206934.t002>

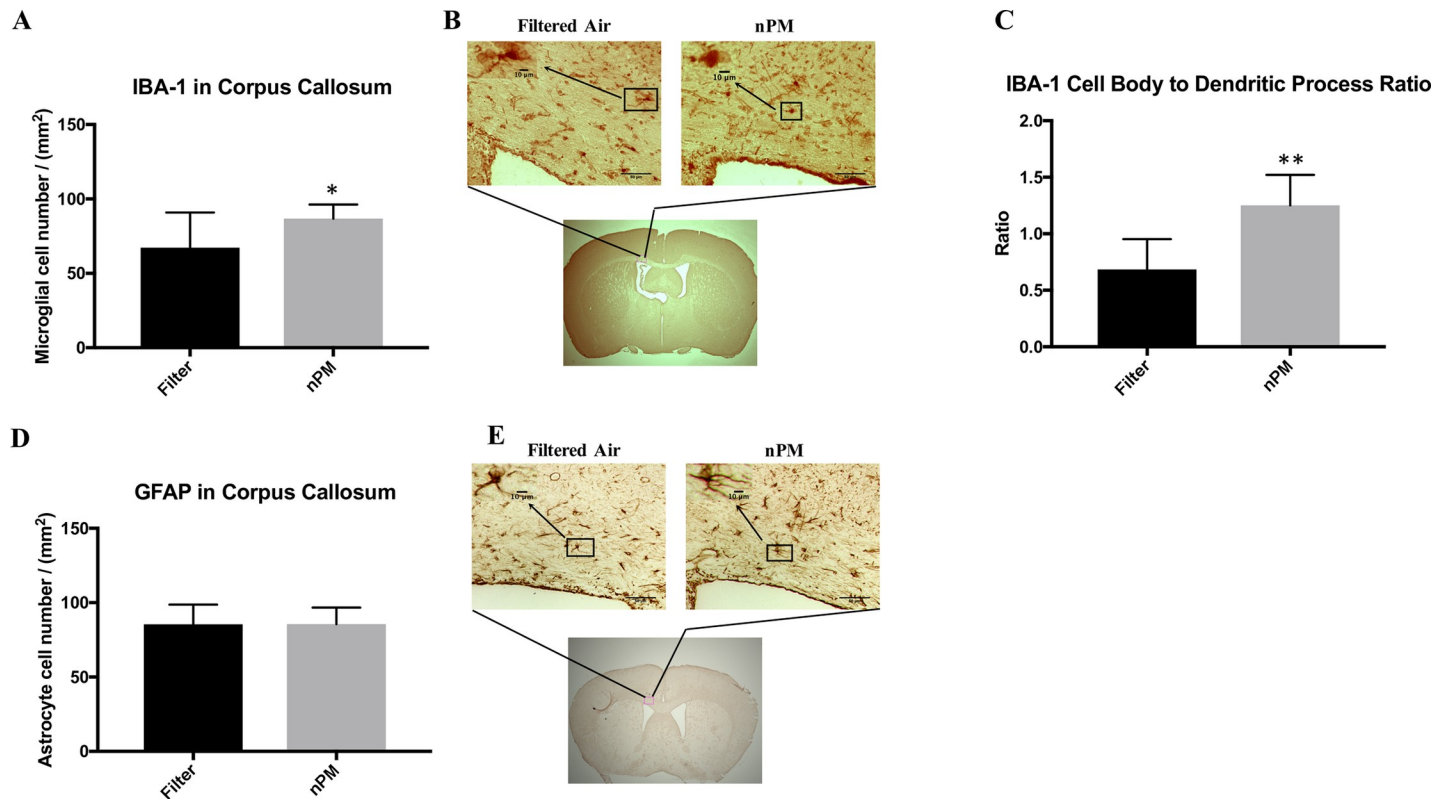


Fig 1. IBA-1 and GFAP staining for reactive glial cells in the medial corpus callosum of mice exposed to filtered air or nanoparticulate matter (nPM). (A) IBA-1 positive cell counts in each experimental group. The nPM group showed significantly greater microglial cell count ($n = 8$) compared to the filtered air group ($n = 8$, $p = 0.047$). * signifies $p < 0.05$. (B) Below; low magnification representation of region analyzed. Above; filtered air and nPM exposed mice stained for IBA-1 in the corpus callosum (40x). The upper left hand corner is a high magnification representation of a single cell. (C) IBA-1 cell body to dendritic process ratio in each experimental group. The nPM cohort had a significantly increased ratio ($n = 8$) compared to the filter group ($n = 8$, $p < 0.001$). ** signifies $p < 0.001$. (D) GFAP positive cell counts in each experimental group. There was no significant difference in astrocyte cell count between groups ($p = 0.983$) (E) Below; low magnification representation of region analyzed. Above; filtered air and nPM exposed mice stained for GFAP in the corpus callosum (40x). The upper left hand corner is a high magnification representation of a single cell. Error bars represent standard deviation. Scale bars are presented on the lower right corner of the images.

<https://doi.org/10.1371/journal.pone.0206934.g001>

Discussion

Clinical and epidemiological investigations have demonstrated strong associations between air pollution particulate matter exposure and neurocognitive injury[26–29]. Both laboratory and translational studies suggest white matter pathology as an anatomic correlate for particulate matter induced neuropsychological decline and advocate an inflammatory mechanism of action. Data from the present study demonstrates increased immunostaining of complement C5 protein, C5a receptor 1 (CD 88), and reactive microglia in the brain white matter (corpus callosum) of mice exposed to nPM. Previously published results suggest that astrocytes, neurons, and microglia express CD88, while only astrocytes and neurons express C5 [30, 31]. Our co-staining analysis suggests that neurons express C5 following air pollution exposure [30, 31]. C5 and GFAP positive cells did not precisely co-localize, so C5 may be produced from astrocytes or the surrounding neurons. Our IBA-1 and C5 immunostaining appeared to co-localize, suggesting either microglial or nearby neuronal expression of C5. C5 may be binding to CD88, resulting in this co-localization or microglia may produce increased levels of C5 following particulate matter exposure.

The C5 complement immunostaining likely results from a local response within the brain rather than upregulation of complement in the blood and entrance through the blood brain

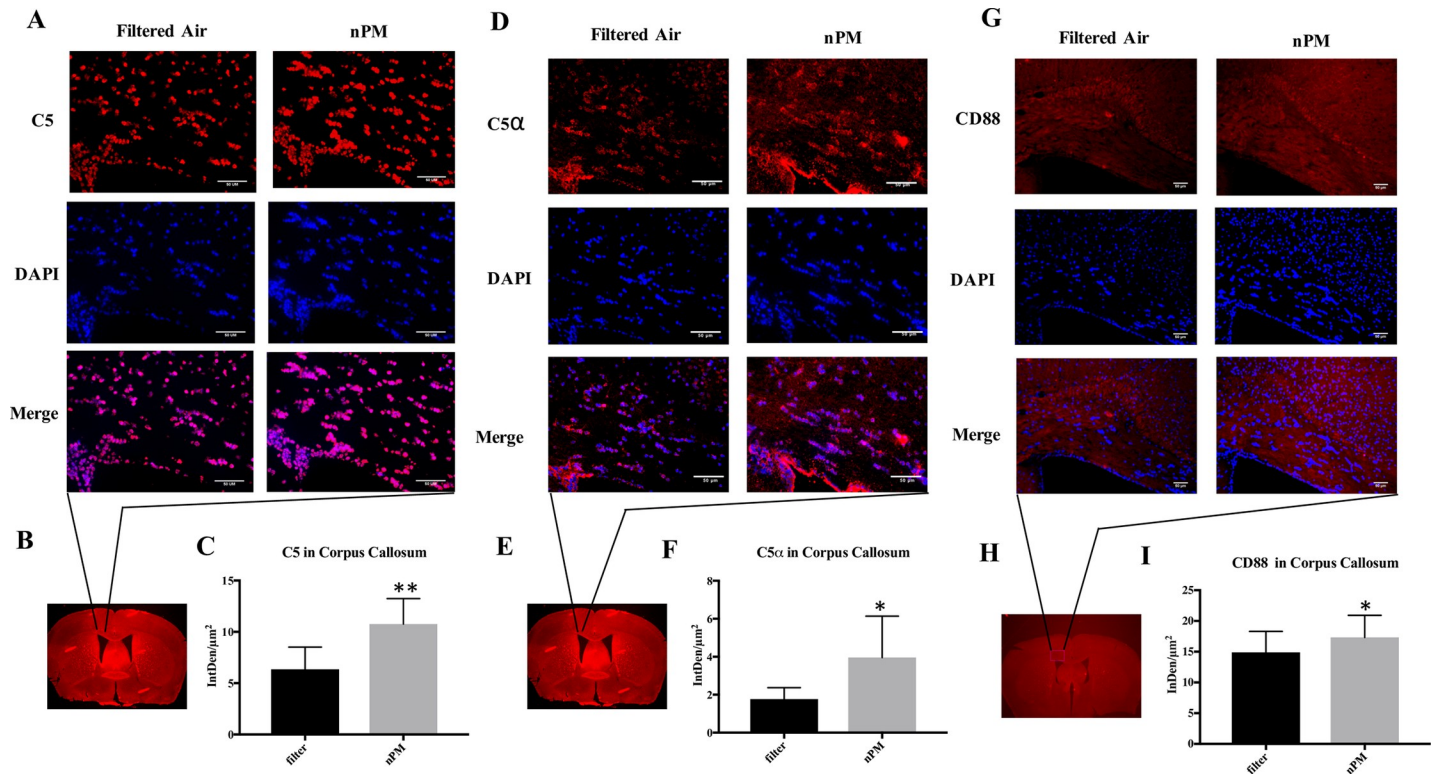


Fig 2. Immunohistochemical analysis of C5, C5 α , and C5a receptor (CD88) in the corpus callosum of animals exposed to filtered air or nanoparticulate matter (nPM). (A) Filtered air (n = 8) or nPM (n = 8) exposed mice stained for C5 (red) in the corpus callosum. Nuclei (DAPI) are stained in blue (400x). (B) Low magnification representation of region analyzed. (C) C5 immunostaining in the corpus callosum was significantly higher in nPM exposed animals compared to the filtered air group (p = 0.001). (D) Filtered air (n = 8) and nPM (n = 8) exposed mice stained for C5 α (red) in the corpus callosum. Nuclei (DAPI) are stained in blue (400x). (E) Low magnification representation of region analyzed. (F) C5 α immunostaining in the corpus callosum of nPM exposed animals was significantly greater than in the filtered air group (p = 0.02). (G) Filtered air (n = 18) and nPM (n = 18) exposed mice stained for CD88 (red) in the corpus callosum. Nuclei (DAPI) are stained in blue (200x). (H) Low magnification representation of region analyzed. (I) CD88 immunostaining in the corpus callosum was significantly higher in nPM exposed animals compared to the filtered air group (p = 0.04). * signifies p < 0.05, ** signifies p \leq 0.001. Error bars represent standard deviation. Scale bars indicate 50 μ m.

<https://doi.org/10.1371/journal.pone.0206934.g002>

barrier. While both C5 and C5 α staining densities were greater in the white matter of mice exposed to nPM, serum C5 levels did not differ between the groups (nPM vs. filtered air). By contrast, TNF-alpha levels were greater in the nPM-exposed mice, supporting a generalized peripheral inflammatory response that is well recognized in the setting of nPM exposure[32–34].

Prior studies demonstrate that diesel exhaust particles activate the complement cascade, particularly the anaphylatoxins, C3a and C5a[35]. Complement modulation (C3 deficiency) has, in turn, been leveraged to decrease exposure-generated inflammation in a murine model of particulate matter-induced lung/ airway hyperresponsiveness[36]. These findings may be generally applicable to other organ systems, including the brain [37]. Our results demonstrate the importance of the complement C5 component in brain white matter inflammation following particulate matter (PM2.5) exposure and specifically focus on the role of microglia. C5a, a chemotaxin for leukocytes and inflammation, induces calcium mobilization and enhances microglial activation[38]. In vitro studies demonstrate transient calcium elevations in microglia on the tissue surface of corpus callosum slices exposed to C5a complement fragments. The investigators observed calcium elevations in microglial cell cultures that were supplemented with complement C5a and C3a[16]. In the resting state, microglia are characterized by small cell bodies, roughly 2–5 μ m in diameter [39, 40] with long, branching processes [24, 41].

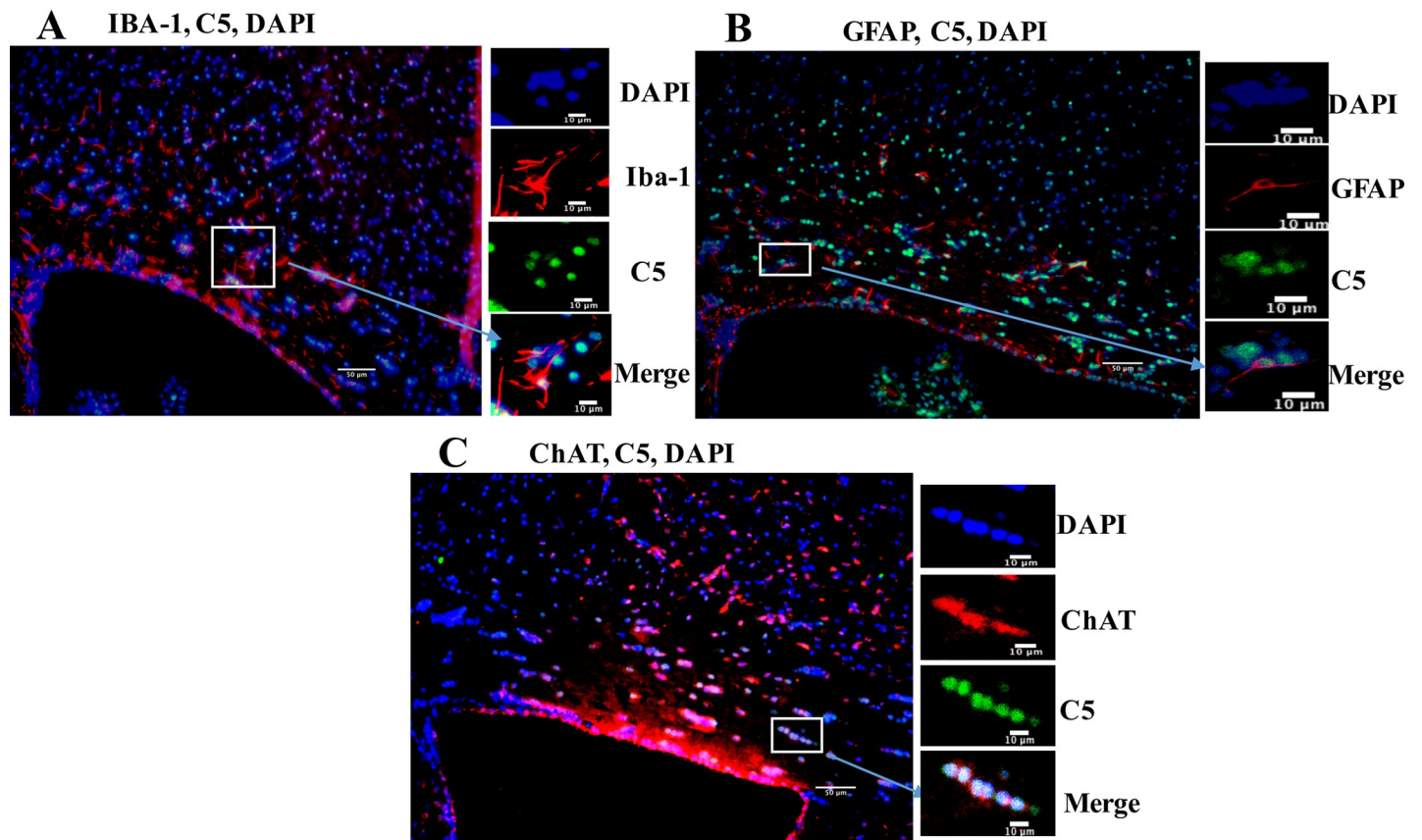


Fig 3. Double immunofluorescence staining of C5 with IBA-1, GFAP, or ChAT in the corpus callosum of animals exposed to nanoparticulate matter (nPM). (A) Co-staining of IBA-1 (red) with C5 (green) in the corpus callosum of a mouse exposed to nPM. Nuclei (DAPI) are stained in blue (200x). (B) Co-staining of GFAP (red) with C5 (green) in the corpus callosum of a mouse exposed to nPM. Nuclei (DAPI) are stained in blue (200x). (C) Co-staining of ChAT (red) with C5 (green) in the corpus callosum of a mouse exposed to nPM. Nuclei (DAPI) are stained in blue (200x). Scale bars are presented on the lower right corner of the images.

<https://doi.org/10.1371/journal.pone.0206934.g003>

When microglia become activated, their cell bodies enlarge and their dendritic processes shorten and thicken [24, 42–44]. In the present study, the increased cell body to dendritic process ratio following air pollution exposure demonstrates a change in microglial morphology, characteristic of activated microglia [24]. The interplay between complement C5 and reactive microglia represents a logical effector of neuroinflammation/ neurotoxicity in our model system, as microglial activation and production of potentially injurious byproducts have been previously demonstrated in the setting of particulate matter exposure. *In vitro* nanosize titanium dioxide exposure stimulates microglial production of reactive oxygen species [45]. These findings are consistent with human data. Autopsy studies of individuals exposed to high levels of air pollution in Mexico City have shown increased CD14 expression, a marker of both resident microglial cells and infiltrating monocytes [46].

Previous data supports a specific role for complement receptor-mediated microglial activation in the setting of diesel exhaust exposure [47, 48]. MAC-1 receptor (complement receptor 3) is expressed exclusively on myeloid lineages, such as microglia. The MAC-1 receptor facilitates reactive microgliosis in response to multiple neurotoxins, including MPTP [49], LPS [50], and alpha-synuclein [51]. Levesque et al have demonstrated that MAC1 is an essential receptor in the process of H₂O₂ production by activated microglia following DEP exposure [47]. Complement component C5a receptor 1 (CD 88) is known to play a critical role in the calcium signaling required for phagocytosis in microglia [52]. It is constitutively expressed on multiple

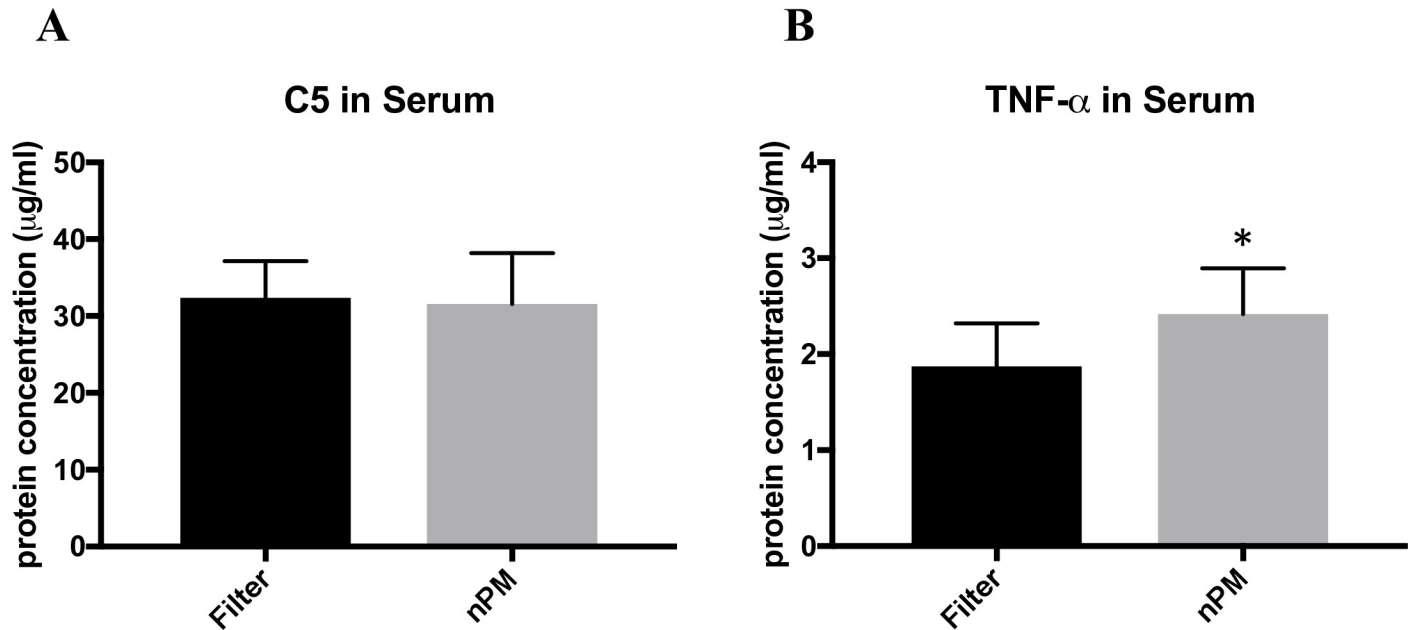


Fig 4. ELISA of serum C5 and TNF-alpha in animals exposed to filtered air or nanoparticulate matter (nPM). Protein concentrations expressed as log values. (A) Serum C5 levels did not differ between the nPM and filtered air groups ($p = 0.785$). (B) TNF-alpha levels were significantly elevated in the nPM group compared to the filtered air group ($p = 0.0419$). * signifies $p < 0.05$. Error bars represent standard deviation.

<https://doi.org/10.1371/journal.pone.0206934.g004>

glial cell lines [14]; however, CNS CD88 expression is influenced by inflammation [53–58], of which particulate matter is a potent source. Mixed neuron-glia cultures exposed to nanosized diesel exhaust particles produce dopaminergic neurotoxicity only in the presence of microglia [59]. Similarly, our data demonstrates a significant increase in corpus callosum CD88 staining and reactive microglia in mice exposed to nPM.

Block et al. suggest that CNS pathology secondary to nPM exposure results from a combination of soluble compounds reaching the brain and peripheral mechanisms involving circulating cytokines from a systemic inflammatory response with the ultimate activation of microglia [7]. In our model system, brain complement C5 deposition could be triggered either by direct nPM toxicity (through the olfactory bulb or blood brain barrier) or a systemic inflammatory response that permeates the blood brain barrier and upregulates complement production via endogenous neurons or glia. Enhanced complement deposition/ upregulation, in turn, may affect microglial migration or activation via CD88 receptors on primarily microglia.

The neuroinflammatory response evident in the corpus callosum in our model appears to be microglia-specific as the nPM cohort showed increases in both cell count and density, as well as a change in morphology, consistent with activated microglia [24]. No significant differences in cell count and cell density of reactive astrocytes were observed between the two groups (nPM and filtered air). The relative lack of astrocytic reactivity in our experiments is supported by a study demonstrating that GFAP levels are unaltered in the brains of rats exposed to combustion products derived from burning of 100% soy bean oil [60]. By contrast, increased GFAP reactivity has been demonstrated following air pollution exposure in the gray matter of the developing brain [61, 62]. Our model focused on the effect of particulate matter in the adult brain, specifically the corpus callosum. The developing brain is more susceptible to injury [63], but also has greater plasticity [64], which may allow for faster recovery. In addition, white matter contains myelin and is suggested to be more susceptible than gray matter to certain types of injury, such as ischemia [65–67]. Calderón-Garcidueñas and colleagues also

found that canines exposed to highly polluted air in Mexico City exhibited increased astrocyte reactivity, particularly in white matter, when compared to canines from a less polluted environment[68]. The air pollution in the Mexico City study had relatively higher ozone, PM_{2.5} and aldehydes than the Los Angeles air sample in our exposure paradigm. Additional environmental factors may have also impacted results, as subjects in the studies by Calderon-Garciduenas et al [34, 46, 68] were not separated directly by air pollution exposure, but rather by geographical location.

White matter damage has been linked to complement upregulation and microglial activation in other experimental systems of neuroinflammation. In the autoimmune encephalitis (EAE) model of multiple sclerosis (MS), microglial cells were found to participate in early stages of myelin destruction[69]. C5 deficient mice demonstrated greater axonal preservation and myelin formation following EAE[70]. In an LPS model of oligodendrocyte death, Li et al. mechanistically demonstrated a role for microglial-derived peroxynitrite, a deleterious byproduct of NADPH oxidase, suggesting that activated microglia could play a critical role in white matter disorders[71]. An investigation of post-mortem brains of healthy children residing in highly polluted environments demonstrated significant staining with CD 68 (a microglial marker) in white matter regions[46]. In an AD transgenic mouse model, Hong et al found that microglia engulf synaptic material in a complement dependent process when exposed to soluble A β oligomers[72]. Taken together, these findings suggest that critical interactions between complement components and activated macrophages/ microglia may play an important role in the white matter response to a host of neuroinflammatory states.

The fact that our cohort consisted of exclusively male mice is a potential limitation of this study. Previous studies have suggested that estrogen may have a protective effect against white matter injury [61, 73]. This effect, particularly in the setting of inflammatory damage, may be explained by microglial expression of estrogen receptors. It is hypothesized that estrogen binding serves to prevent microglial activation and resulting injury[74]. Future studies investigating air pollution exposure in female mice can be leveraged to assess the sex differences and estrogen's role in white matter damage. The potential effects of the anesthetic regimen at the time of euthanasia must also be considered when interpreting the cellular data. Given the findings of previous studies[75–77], it is unlikely that ketamine-xylazine anesthesia significantly altered the levels of inflammation.

The size and chemical composition of the particulate matter used in this experiment are comparable to that present in an urban area. nPM exposure levels of approximately 330 $\mu\text{g}/\text{m}^3$ are roughly twice the levels present on busy Los Angeles freeways with a high volume of diesel trucks [21, 78, 79]. This concentration is similar to those used in previous studies [42, 60, 80].

In conclusion, this study demonstrates increased complement C5 immunostaining and microglial activation secondary to nPM exposure. The complement upregulation appears to be localized to the brain, as serum C5 levels did not differ between nPM and filtered air-exposed mice. These findings indicate that interaction between the complement anaphylatoxins (particularly C5a) and activated microglia may play an important role in white matter injury following nPM exposure.

Supporting information

S1 File. IBA-1 Cell count and density dataset.
(XLSX)

S2 File. IBA-1 Cell body and dendritic process size datasheet.
(XLSX)

S3 File. GFAP cell count and density dataset.

(XLSX)

S4 File. C5 and C5 α density dataset.

(XLSX)

S5 File. CD88 density dataset.

(XLSX)

S6 File. Serum C5 and serum TNF-alpha dataset.

(XLSX)

Author Contributions

Conceptualization: Constantinos Sioutas, Todd E. Morgan, Caleb E. Finch, William J. Mack.**Formal analysis:** Robin Babadjouni, Arati Patel, Qinghai Liu, Kristina Shkirkova, Krista Lamorie-Foote, Michelle Connor, Drew M. Hodis, Hank Cheng.**Methodology:** Michelle Connor, Constantinos Sioutas, Todd E. Morgan, Caleb E. Finch, William J. Mack.**Project administration:** Robin Babadjouni, Arati Patel, Qinghai Liu, Kristina Shkirkova, Krista Lamorie-Foote, Drew M. Hodis, Hank Cheng.**Writing – review & editing:** Robin Babadjouni, Arati Patel, Constantinos Sioutas, Todd E. Morgan, Caleb E. Finch, William J. Mack.

References

1. Morgan TE, Davis DA, Iwata N, Tanner JA, Snyder D, Ning Z, et al. Glutamatergic neurons in rodent models respond to nanoscale particulate urban air pollutants in vivo and in vitro. *Environmental health perspectives*. 2011; 119(7):1003. <https://doi.org/10.1289/ehp.1002973> PMID: 21724521
2. Calderón-Garcidueñas L, de la Monte SM. Apolipoprotein E4, Gender, Body Mass Index, Inflammation, Insulin Resistance, and Air Pollution Interactions: Recipe for Alzheimer's Disease Development in Mexico City Young Females. *Journal of Alzheimer's Disease*. 2017; 58(3):613–30. <https://doi.org/10.3233/JAD-161299> PMID: 28527212
3. Chen JC, Wang X, Wellenius GA, Serre ML, Driscoll I, Casanova R, et al. Ambient air pollution and neurotoxicity on brain structure: Evidence from women's health initiative memory study. *Ann Neurol*. 2015; 78(3):466–76. <https://doi.org/10.1002/ana.24460> PMID: 26075655
4. Power MC, Weisskopf MG, Alexeeff SE, Coull BA, Spiro A, 3rd, Schwartz J. Traffic-related air pollution and cognitive function in a cohort of older men. *Environ Health Perspect*. 2011; 119(5):682–7. <https://doi.org/10.1289/ehp.1002767> PMID: 21172758
5. Wellenius GA, Boyle LD, Coull BA, Milberg WP, Gryparis A, Schwartz J, et al. Residential proximity to nearest major roadway and cognitive function in community-dwelling seniors: results from the MOBILIZE Boston Study. *J Am Geriatr Soc*. 2012; 60(11):2075–80. <https://doi.org/10.1111/j.1532-5415.2012.04195.x> PMID: 23126566
6. Woodward NC, Pakbin P, Saffari A, Shirmohammadi F, Haghani A, Sioutas C, et al. Traffic-related air pollution impact on mouse brain accelerates myelin and neuritic aging changes with specificity for CA1 neurons. *Neurobiol Aging*. 2017; 53:48–58. <https://doi.org/10.1016/j.neurobiolaging.2017.01.007> PMID: 28212893
7. Block ML, Calderón-Garcidueñas L. Air pollution: mechanisms of neuroinflammation and CNS disease. *Trends in neurosciences*. 2009; 32(9):506–16. <https://doi.org/10.1016/j.tins.2009.05.009> PMID: 19716187
8. Schafer DP, Stevens B. Microglia function in central nervous system development and plasticity. *Cold Spring Harbor perspectives in biology*. 2015; 7(10):a020545. <https://doi.org/10.1101/cshperspect.a020545> PMID: 26187728
9. Trapp BD, Bö L, Mörk S, Chang A. Pathogenesis of tissue injury in MS lesions. *Journal of neuroimmunology*. 1999; 98(1):49–56. PMID: 10426362

10. Haynes RL, Folkerth RD, Keefe RJ, Sung I, Swzeda LI, Rosenberg PA, et al. Nitrosative and oxidative injury to premyelinating oligodendrocytes in periventricular leukomalacia. *Journal of Neuropathology & Experimental Neurology*. 2003; 62(5):441–50.
11. Moisse K, Welch I, Hill T, Volkening K, Strong MJ. Transient middle cerebral artery occlusion induces microglial priming in the lumbar spinal cord: a novel model of neuroinflammation. *Journal of neuroinflammation*. 2008; 5(1):29.
12. Barnum S. Complement biosynthesis in the central nervous system. *Critical Reviews in Oral Biology & Medicine*. 1995; 6(2):132–46.
13. Walker D, Kim S, McGeer P. Complement and cytokine gene expression in cultured microglia derived from postmortem human brains. *Journal of neuroscience research*. 1995; 40(4):478–93. <https://doi.org/10.1002/jnr.490400407> PMID: 7616608
14. Gasque P, Singhrao SK, Neal JW, Götz O, Morgan BP. Expression of the receptor for complement C5a (CD88) is up-regulated on reactive astrocytes, microglia, and endothelial cells in the inflamed human central nervous system. *The American journal of pathology*. 1997; 150(1):31. PMID: 9006319
15. Lacy M, Jones J, Whittemore SR, Haviland DL, Wetsel RA, Barnum SR. Expression of the receptors for the C5a anaphylatoxin, interleukin-8 and FMLP by human astrocytes and microglia. *Journal of neuroimmunology*. 1995; 61(1):71–8. PMID: 7560015
16. Möller T, Nolte C, Burger R, Verkhatsky A, Kettenmann H. Mechanisms of C5a and C3a complement fragment-induced [Ca²⁺]_i signaling in mouse microglia. *Journal of Neuroscience*. 1997; 17(2):615–24. PMID: 8987784
17. Zajicek J, Wing M, Scolding N, Compston D. Interactions between oligodendrocytes and microglia. *Brain*. 1992; 115(6):1611–31.
18. Woodward NC, Levine MC, Haghani A, Shirmohammadi F, Saffari A, Sioutas C, et al. Toll-like receptor 4 in glial inflammatory responses to air pollution in vitro and in vivo. *Journal of neuroinflammation*. 2017; 14(1):84. <https://doi.org/10.1186/s12974-017-0858-x> PMID: 28410596
19. Misra C, Kim S, Shen S, Sioutas C. A high flow rate, very low pressure drop impactor for inertial separation of ultrafine from accumulation mode particles. *Journal of Aerosol Science*. 2002; 33(5):735–52.
20. Biran R, Tang Y-Z, Brook J, Vincent R, Keeler G. Aqueous extraction of airborne particulate matter collected on hi-vol Teflon filters. *International journal of environmental analytical chemistry*. 1996; 63(4):315–22.
21. Fruin S, Westerdahl D, Sax T, Sioutas C, Fine P. Measurements and predictors of on-road ultrafine particle concentrations and associated pollutants in Los Angeles. *Atmospheric Environment*. 2008; 42(2):207–19.
22. Li R, Navab M, Pakbin P, Ning Z, Navab K, Hough G, et al. Ambient ultrafine particles alter lipid metabolism and HDL anti-oxidant capacity in LDLR-null mice. *Journal of lipid research*. 2013; 54(6):1608–15. <https://doi.org/10.1194/jlr.M035014> PMID: 23564731
23. Davis DA, Bortolato M, Godar SC, Sander TK, Iwata N, Pakbin P, et al. Prenatal exposure to urban air nanoparticles in mice causes altered neuronal differentiation and depression-like responses. *PloS one*. 2013; 8(5):e64128. <https://doi.org/10.1371/journal.pone.0064128> PMID: 23734187
24. Hovens IB, van Leeuwen BL, Nyakas C, Heineman E, van der Zee EA, Schoemaker RG. Postoperative cognitive dysfunction and microglial activation in associated brain regions in old rats. *Neurobiol Learn Mem*. 2015; 118:74–9. <https://doi.org/10.1016/j.nlm.2014.11.009> PMID: 25460037
25. German DC, Bruce G, Hersh LB. Immunohistochemical staining of cholinergic neurons in the human brain using a polyclonal antibody to human choline acetyltransferase. *Neurosci Lett*. 1985; 61(1–2):1–5. PMID: 3908999
26. Kilburn KH. Effects of diesel exhaust on neurobehavioral and pulmonary functions. *Arch Environ Health*. 2000; 55(1):11–7. <https://doi.org/10.1080/00039890009603379> PMID: 10735514
27. Ranft U, Schikowski T, Sugiri D, Krutmann J, Krämer U. Long-term exposure to traffic-related particulate matter impairs cognitive function in the elderly. *Environmental research*. 2009; 109(8):1004–11. <https://doi.org/10.1016/j.envres.2009.08.003> PMID: 19733348
28. Power MC, Weisskopf MG, Alexeeff SE, Coull BA, Spiro III A, Schwartz J. Traffic-related air pollution and cognitive function in a cohort of older men. *Environmental health perspectives*. 2011; 119(5):682. <https://doi.org/10.1289/ehp.1002767> PMID: 21172758
29. Calderón-Garcidueñas L, Mora-Tiscareño A, Ontiveros E, Gómez-Garza G, Barragán-Mejía G, Broadway J, et al. Air pollution, cognitive deficits and brain abnormalities: a pilot study with children and dogs. *Brain and cognition*. 2008; 68(2):117–27. <https://doi.org/10.1016/j.bandc.2008.04.008> PMID: 18550243
30. Veerhuis R, Nielsen HM, Tenner AJ. Complement in the brain. *Mol Immunol*. 2011; 48(14):1592–603. <https://doi.org/10.1016/j.molimm.2011.04.003> PMID: 21546088

31. Farkas I, Baranyi L, Takahashi M, Fukuda A, Liposits Z, Yamamoto T, et al. A neuronal C5a receptor and an associated apoptotic signal transduction pathway. *J Physiol*. 1998; 507 (Pt 3):679–87.
32. Tamagawa E, Bai N, Morimoto K, Gray C, Mui T, Yatera K, et al. Particulate matter exposure induces persistent lung inflammation and endothelial dysfunction. *American Journal of Physiology-Lung Cellular and Molecular Physiology*. 2008; 295(1):L79–L85. <https://doi.org/10.1152/ajplung.00048.2007> PMID: 18469117
33. Mutlu GM, Green D, Bellmeyer A, Baker CM, Burgess Z, Rajamannan N, et al. Ambient particulate matter accelerates coagulation via an IL-6–dependent pathway. *The Journal of clinical investigation*. 2007; 117(10):2952–61. <https://doi.org/10.1172/JCI30639> PMID: 17885684
34. Calderón-Garcidueñas L, Engle R, Mora-Tiscareño A, Styner M, Gómez-Garza G, Zhu H, et al. Exposure to severe urban air pollution influences cognitive outcomes, brain volume and systemic inflammation in clinically healthy children. *Brain and cognition*. 2011; 77(3):345–55. <https://doi.org/10.1016/j.bandc.2011.09.006> PMID: 22032805
35. Kanemitsu H, Nagasawa S, Sagai M, MORI Y. Complement activation by diesel exhaust particles (DEP). *Biological and Pharmaceutical Bulletin*. 1998; 21(2):129–32. PMID: 9514606
36. Walters DM, Breyse PN, Wills-Karp M. Ambient urban Baltimore particulate-induced airway hyperresponsiveness and inflammation in mice. *American journal of respiratory and critical care medicine*. 2001; 164(8):1438–43.
37. Kramer U, Herder C, Sugiri D, Strassburger K, Schikowski T, Ranft U, et al. Traffic-related air pollution and incident type 2 diabetes: results from the SALIA cohort study. *Environ Health Perspect*. 2010; 118(9):1273–9. <https://doi.org/10.1289/ehp.0901689> PMID: 20504758
38. Crehan H, Hardy J, Pocock J. Microglia, Alzheimer's disease, and complement. *International Journal of Alzheimer's Disease*. 2012;2012.
39. Shapiro LA, Perez ZD, Foresti ML, Arisi GM, Ribak CE. Morphological and ultrastructural features of Iba1-immunolabeled microglial cells in the hippocampal dentate gyrus. *Brain Res*. 2009; 1266:29–36. <https://doi.org/10.1016/j.brainres.2009.02.031> PMID: 19249294
40. Peters A, Palay SL, Webster Hd. *The fine structure of the nervous system: neurons and their supporting cells*. 3rd ed. New York: Oxford University Press; 1991. xviii, 494 p. p.
41. Ransohoff RM, Perry VH. Microglial physiology: unique stimuli, specialized responses. *Annu Rev Immunol*. 2009; 27:119–45. <https://doi.org/10.1146/annurev.immunol.021908.132528> PMID: 19302036
42. Cheng H, Saffari A, Sioutas C, Forman HJ, Morgan TE, Finch CE. Nanoscale Particulate Matter from Urban Traffic Rapidly Induces Oxidative Stress and Inflammation in Olfactory Epithelium with Concomitant Effects on Brain. *Environ Health Perspect*. 2016; 124(10):1537–46. <https://doi.org/10.1289/EHP134> PMID: 27187980
43. Eggen BJ, Raj D, Hanisch UK, Boddeke HW. Microglial phenotype and adaptation. *J Neuroimmune Pharmacol*. 2013; 8(4):807–23. <https://doi.org/10.1007/s11481-013-9490-4> PMID: 23881706
44. Kettenmann H, Hanisch UK, Noda M, Verkhratsky A. Physiology of microglia. *Physiol Rev*. 2011; 91(2):461–553. <https://doi.org/10.1152/physrev.00011.2010> PMID: 21527731
45. Long TC, Tajuba J, Sama P, Saleh N, Swartz C, Parker J, et al. Nanosize titanium dioxide stimulates reactive oxygen species in brain microglia and damages neurons in vitro. *Environmental Health Perspectives*. 2007;1631–7. <https://doi.org/10.1289/ehp.10216> PMID: 18007996
46. Calderón-Garcidueñas L, Solt AC, Henríquez-Roldán C, Torres-Jardón R, Nuse B, Herritt L, et al. Long-term air pollution exposure is associated with neuroinflammation, an altered innate immune response, disruption of the blood-brain barrier, ultrafine particulate deposition, and accumulation of amyloid β -42 and α -synuclein in children and young adults. *Toxicologic pathology*. 2008; 36(2):289–310. <https://doi.org/10.1177/0192623307313011> PMID: 18349428
47. Levesque S, Taetzsch T, Lull ME, Johnson JA, McGraw C, Block ML. The role of MAC1 in diesel exhaust particle-induced microglial activation and loss of dopaminergic neuron function. *Journal of neurochemistry*. 2013; 125(5):756–65. <https://doi.org/10.1111/jnc.12231> PMID: 23470120
48. Levesque S, Taetzsch T, Lull ME, Kodavanti U, Stadler K, Wagner A, et al. Diesel exhaust activates and primes microglia: air pollution, neuroinflammation, and regulation of dopaminergic neurotoxicity. *Environmental health perspectives*. 2011; 119(8):1149. <https://doi.org/10.1289/ehp.1002986> PMID: 21561831
49. Hu X, Zhang D, Pang H, Caudle WM, Li Y, Gao H, et al. Macrophage antigen complex-1 mediates reactive microgliosis and progressive dopaminergic neurodegeneration in the MPTP model of Parkinson's disease. *The Journal of Immunology*. 2008; 181(10):7194–204. PMID: 18981141
50. Wright SD, Tobias PS, Ulevitch RJ, Ramos RA. Lipopolysaccharide (LPS) binding protein opsonizes LPS-bearing particles for recognition by a novel receptor on macrophages. *J Exp Med*. 1989; 170(4):1231–41. PMID: 2477488

51. Zhang W, Dallas S, Zhang D, Guo JP, Pang H, Wilson B, et al. Microglial PHOX and Mac-1 are essential to the enhanced dopaminergic neurodegeneration elicited by A30P and A53T mutant alpha-synuclein. *Glia*. 2007; 55(11):1178–88. <https://doi.org/10.1002/glia.20532> PMID: 17600340
52. Hoffmann A, Kann O, Ohlemeyer C, Hanisch U-K, Kettenmann H. Elevation of basal intracellular calcium as a central element in the activation of brain macrophages (microglia): suppression of receptor-evoked calcium signaling and control of release function. *Journal of Neuroscience*. 2003; 23(11):4410–9. PMID: 12805281
53. Woodruff TM, Ager RR, Tenner AJ, Noakes PG, Taylor SM. The role of the complement system and the activation fragment C5a in the central nervous system. *Neuromolecular medicine*. 2010; 12(2):179–92. <https://doi.org/10.1007/s12017-009-8085-y> PMID: 19763906
54. Stahel PF, Kariya K, Shohami E, Barnum SR, Eugster H-P, Trentz O, et al. Intracerebral complement C5a receptor (CD88) expression is regulated by TNF and lymphotoxin- α following closed head injury in mice. *Journal of neuroimmunology*. 2000; 109(2):164–72. PMID: 10996218
55. Stahel PF, Frei K, Eugster H-P, Fontana A, Hummel KM, Wetsel RA, et al. TNF-alpha-mediated expression of the receptor for anaphylatoxin C5a on neurons in experimental *Listeria meningoencephalitis*. *The Journal of Immunology*. 1997; 159(2):861–9. PMID: 9218605
56. Van Beek J, Bernaudin M, Petit E, Gasque P, Nouvelot A, MacKenzie ET, et al. Expression of receptors for complement anaphylatoxins C3a and C5a following permanent focal cerebral ischemia in the mouse. *Experimental neurology*. 2000; 161(1):373–82. <https://doi.org/10.1006/exnr.1999.7273> PMID: 10683302
57. Woodruff TM, Crane JW, Proctor LM, Buller KM, Shek AB, De Vos K, et al. Therapeutic activity of C5a receptor antagonists in a rat model of neurodegeneration. *The FASEB Journal*. 2006; 20(9):1407–17. <https://doi.org/10.1096/fj.05-5814com> PMID: 16816116
58. Woodruff TM, Costantini KJ, Crane JW, Atkin JD, Monk PN, Taylor SM, et al. The complement factor C5a contributes to pathology in a rat model of amyotrophic lateral sclerosis. *The Journal of Immunology*. 2008; 181(12):8727–34. PMID: 19050293
59. Block M, Wu X, Pei Z, Li G, Wang T, Qin L, et al. Nanometer size diesel exhaust particles are selectively toxic to dopaminergic neurons: the role of microglia, phagocytosis, and NADPH oxidase. *The FASEB Journal*. 2004; 18(13):1618–20. <https://doi.org/10.1096/fj.04-1945fje> PMID: 15319363
60. Finch G, Hobbs C, Blair L, Barr E, Hahn F, Jaramillo R, et al. Effects of subchronic inhalation exposure of rats to emissions from a diesel engine burning soybean oil-derived biodiesel fuel. *Inhalation toxicology*. 2002; 14(10):1017–48. <https://doi.org/10.1080/08958370290084764> PMID: 12396409
61. Allen JL, Oberdorster G, Morris-Schaffer K, Wong C, Klocke C, Sobolewski M, et al. Developmental neurotoxicity of inhaled ambient ultrafine particle air pollution: Parallels with neuropathological and behavioral features of autism and other neurodevelopmental disorders. *Neurotoxicology*. 2017; 59:140–54. <https://doi.org/10.1016/j.neuro.2015.12.014> PMID: 26721665
62. Onoda A, Takeda K, Umezawa M. Dose-dependent induction of astrocyte activation and reactive astrogliosis in mouse brain following maternal exposure to carbon black nanoparticle. *Part Fibre Toxicol*. 2017; 14(1):4. <https://doi.org/10.1186/s12989-017-0184-6> PMID: 28148272
63. Costa LG, Aschner M, Vitalone A, Syversen T, Soldin OP. Developmental neuropathology of environmental agents. *Annu Rev Pharmacol Toxicol*. 2004; 44:87–110. <https://doi.org/10.1146/annurev.pharmtox.44.101802.121424> PMID: 14744240
64. Johnston MV, Ishida A, Ishida WN, Matsushita HB, Nishimura A, Tsuji M. Plasticity and injury in the developing brain. *Brain Dev*. 2009; 31(1):1–10. <https://doi.org/10.1016/j.braindev.2008.03.014> PMID: 18490122
65. Ransom BR, Goldberg MP, Arai K, Baltan S. *White Matter Pathophysiology. Stroke: Pathophysiology, Diagnosis, and Management*; Elsevier Inc.; 2015.
66. Pantoni L, Garcia JH, Gutierrez JA. Cerebral white matter is highly vulnerable to ischemia. *Stroke*. 1996; 27(9):1641–6; discussion 7. PMID: 8784142
67. Wang Y, Liu G, Hong D, Chen F, Ji X, Cao G. White matter injury in ischemic stroke. *Progress in neurobiology*. 2016; 141:45–60. <https://doi.org/10.1016/j.pneurobio.2016.04.005> PMID: 27090751
68. Calderón-Garcidueñas L, Azzarelli B, Acuna H, Garcia R, Gambling TM, Osnaya N, et al. Air pollution and brain damage. *Toxicologic pathology*. 2002; 30(3):373–89. <https://doi.org/10.1080/01926230252929954> PMID: 12051555
69. Sriram S, Rodríguez M. Indictment of the microglia as the villain in multiple sclerosis. *Neurology*. 1997; 48(2):464–70. PMID: 9040740
70. Cudrici C, Niculescu T, Niculescu F, Shin ML. Oligodendrocyte cell death in pathogenesis of multiple sclerosis: Protection of oligodendrocytes from apoptosis by complement. *Journal of rehabilitation research and development*. 2006; 43(1):123. PMID: 16847778

71. Li J, Baud O, Vartanian T, Volpe JJ, Rosenberg PA. Peroxynitrite generated by inducible nitric oxide synthase and NADPH oxidase mediates microglial toxicity to oligodendrocytes. *Proceedings of the National Academy of Sciences of the United States of America*. 2005; 102(28):9936–41. <https://doi.org/10.1073/pnas.0502552102> PMID: 15998743
72. Hong S, Beja-Glasser VF, Nfonoyim BM, Frouin A, Li S, Ramakrishnan S, et al. Complement and microglia mediate early synapse loss in Alzheimer mouse models. *Science*. 2016; 352(6286):712–6. <https://doi.org/10.1126/science.aad8373> PMID: 27033548
73. Dominguez R, Zitting M, Liu Q, Patel A, Babadjouni R, Hodis DM, et al. Estradiol Protects White Matter of Male C57BL6J Mice against Experimental Chronic Cerebral Hypoperfusion. *J Stroke Cerebrovasc Dis*. 2018; 27(7):1743–51. <https://doi.org/10.1016/j.jstrokecerebrovasdis.2018.01.030> PMID: 29602614
74. Villa A, Vegeto E, Poletti A, Maggi A. Estrogens, Neuroinflammation, and Neurodegeneration. *Endocr Rev*. 2016; 37(4):372–402. <https://doi.org/10.1210/er.2016-1007> PMID: 27196727
75. Al-Mousawi AM, Kulp GA, Branski LK, Kraft R, Mecott GA, Williams FN, et al. Impact of anesthesia, analgesia, and euthanasia technique on the inflammatory cytokine profile in a rodent model of severe burn injury. *Shock*. 2010; 34(3):261–8. PMID: 20803788
76. DeWalt GJ, Mahajan B, Foster AR, Thompson LDE, Martini AA, Schmidt EV, et al. Region-specific alterations in astrocyte and microglia morphology following exposure to blasts in the mouse hippocampus. *Neurosci Lett*. 2018; 664:160–6. <https://doi.org/10.1016/j.neulet.2017.11.016> PMID: 29133177
77. Ward JL, Harting MT, Cox CS Jr., Mercer DW. Effects of ketamine on endotoxin and traumatic brain injury induced cytokine production in the rat. *J Trauma*. 2011; 70(6):1471–9. <https://doi.org/10.1097/TA.0b013e31821c38bd> PMID: 21817985
78. Kam W, Liacos JW, Schauer JJ, Delfino RJ, Sioutas C. On-road emission factors of PM pollutants for light-duty vehicles (LDVs) based on urban street driving conditions. *Atmospheric environment*. 2012; 61:378–86.
79. Kam W, Liacos J, Schauer J, Delfino R, Sioutas C. Size-segregated composition of particulate matter (PM) in major roadways and surface streets. *Atmospheric environment*. 2012; 55:90–7.
80. Campbell A, Oldham M, Becaria A, Bondy SC, Meacher D, Sioutas C, et al. Particulate matter in polluted air may increase biomarkers of inflammation in mouse brain. *Neurotoxicology*. 2005; 26(1):133–40. <https://doi.org/10.1016/j.neuro.2004.08.003> PMID: 15527881